International Journal of Science and Technology

http://www.ejournalofsciences.org

Functional Fitting of Monte Carlo Output Parameters for the Nucletron Pulsed Dose Rate Brachytherapy Source

M. Pokoo – Aikins[1,2], A. Kyere[2] , F. Hasford[1,2], M. Boadu[1,2], G.F. Acquah[2] and E. K. Sosu[1,2]
[1]Radiological and Medical Sciences and Research Institute, Ghana Atomic Energy Commission,
P.O. Box LG 80, Legon - Accra,Ghana.
[2]Graduate School of Nuclear and Allied Sciences, University of Ghana, P.O. Box AE 1, Atomic Energy, Ghana.

ABSTRACT

The current brachytherapy treatment planning system employs the TG 43 formalism proposed by the American Association of Medical Physicists in Medicine (AAPM). The TG 43 uses dose rate tables which assume cylindrical symmetry of the sources, and the medium in which the calculation is made is water equivalent, with no modification for different heterogeneities and no account for applicator attenuation. The dose rate tables sometimes require interpolation and extrapolation, which may lead to uncertainties in dose calculations. This work aims to fit functions for the Monte Carlo output parameters generated by Lliso et al. (2001) [10], in the quest to develop a functional form which will reduce the number of independent variables, reduce the uncertainties in dose calculation distribution around the Nucletron pulsed dose rate (PDR) ^{192}Ir brachytherapy source, and hence to facilitate implementation of the TG 43 formalism. The fitting and verifications were done using different software of the computer, e.g., Matlab, MS word, MS excel. We used Matlab fitting tool to fit the functions for the Nucletron PDR MC output parameters generated by Lliso et al. The accuracy of the fit functional form obtained was verified by comparing the dose rate distribution per unit air kerma strength obtained from the fit, to the dose rate distribution per unit air kerma strength obtained directly for the work of Lliso. For the absolute dose rate error calculations, deviation and mean were used. The average discrepancies in the dose rate per unit air kerma strength (in $cGyh^{-1}U^{-1}$) obtained from the fit were all found to be less than 1 %, within the TG – 43 recommended statistical uncertainty limit $\leq 2\%$. The results from this study, it is hoped can be used as input data in TPS, and to verify calculations of TPS for precise brachytherapy treatment planning.

Keywords: *Brachytherapy, Monte Carlo, functional fitting, TG 43 formalism.*

I. INTRODUCTION

Pulsed dose rate treatment has been a preferred brachytherapy modality which combines physical advantages of high dose rate (HDR) brachytherapy technology with the radiobiological advantages of low dose rate (LDR) brachytherapy. The most complete formalism available today for PDR treatments is the TG 43 formalism. However, the TG 43 formalism has clinically relevant limitations for calculating patient dose. It uses dose rate tables which sometimes require interpolation and extrapolation, and the medium in which the calculation is made is water equivalent, with no modification for different heterogeneities and no account for applicator attenuation [1, 2].

Monte Carlo calculations, in which the phantom medium is replaced by water, can be used for such corrections. MC calculations have been used as a reliable tool in determining dose distribution around brachytherapy sources. Heterogeneities effects are included only when Monte Carlo calculations are used [3, 4].

A number of publications about dosimetric data of the commonly used sources are available. In their publication, Williamson et al. (1995) [5] employ a Monte Carlo code to calculate dose-rate distributions around the Nucletron HDR ^{192} Ir source and the PDR ^{192} Ir source. The results are presented as 2-D Cartesian lookup tables and in the formalism recommended by the TG 43. [6]. Wang et al. (1998) [7] calculated basic dosimetry data for a VariSource HDR ^{192}Ir source and Daskalov et al. [8] published a similar study for the microSelectron HDR ^{192}Ir source.

Several treatment planning systems (TPSs) rely on functional fits of the radial dose function and anisotropy function data in dose calculation and distribution around the brachytherapy source. These are necessary to eliminate noisy outliers, smooth the original data obtained and to enable the calculation of lookup tables to support the treatment planning.

This study aims at fitting functions for the MC output parameters generated by Lliso et al. (2001) [10], by representing the MC dosimetric quantities as TG 43 modified parameters in the quest to develop a functional form which will reduce the number of independent variables. This development is to make handling data easier within the treatment planning system, avoiding the use of tabulated data for the Nucletron PDR ^{192}Ir source.

II. SUBJECTS AND METHODS

The data plotting and the polynomial fit of the MC modified TG 43 output parameters were produced using the method of least squares based on the computer MATLAB Curve Fitting Toolbox version 2.0 (R2009a).

A Nucletron PDR ^{192}Ir cylindrical source with total length of 3.1 mm and diameter of 1.1 mm (active source length of 0.6mm and diameter 0.6 mm with stainless steel encapsulation), distance from active end to tip of 0.55 mm was used in all calculations presented in this study. The source is used in a MicroSelectron PDR afterloading system, and is moved in a "step-forward" manner through an applicator. The geometric dimensions of the Nucletron PDR ^{192}Ir cylindrical source are retrieved from the ESTRO booklet [1], and illustrated in Figure 1.

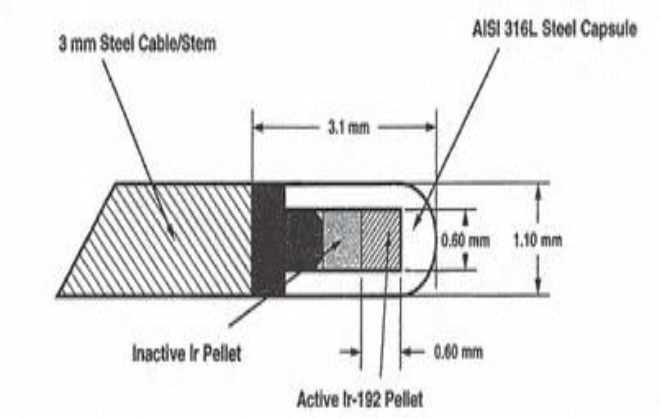

Figure 1: Schematic diagram of the Nucletron PDR ^{192}Ir source used in this study.

In this study, the TG 43 formalism (equation 1) is rewritten in such a way that the anisotropy function F(r,θ) and the radial function g(r) are hybridized into a single function f(r,θ) as given by Acquah et al. (2012) [9] in equation 2.

$$\dot{D}(r,\theta) = S_K \Lambda \frac{G(r,\theta)}{G(r_0,\theta_0)} g(r) F(r,\theta) \quad (1)$$

$$\dot{D}(r,\theta) = S_K \Lambda \frac{G(r,\theta)}{G(r_0,\theta_0)} f(r,\theta) \quad (2)$$

where $f(r,\theta) = g(r) \times F(r,\theta)$ (3)

Hence the number of parameters used in absorbed dose rate calculation at any point is reduced in equation 2. This provides an improvement in the accuracy in absorbed dose rate calculation, and the data fitting.

The hybridized function in equation 3 denotes the normalised dose rate at the reference point. In this equation, the effect of geometry factor has also been removed to improve the efficiency of fitting.

For the purpose of this study, the formula by Lliso et al. (2001) [10] was embraced as the standard for dose calculations around the Nucletron PDR ^{192}Ir source. Lliso et al. have proved that fitting the dosimetric parameters was in excellent agreement with data obtained using the Monte Carlo output parameters, and the uncertainties due to the fitting procedure was found to be very small. The absolute value of relative deviation obtained for the PDR Nucletron source is 0.4% for both $F(r\theta)$ and g(r) respectively, suggesting that the average fit error is less than 1% in all cases [10].

According to Lliso et al. [10], the anisotropy function and the radial function are given as shown in equations 4 and 5 respectively.

$$F(r,\theta) = K(r) + \frac{a(r)\left(\frac{\theta}{\pi}\right)^{e(r)}}{1+b(r)\left(\frac{\theta}{\pi}\right)^{e(r)}} + \frac{a'(r)\left(1-\frac{\theta}{\pi}\right)^{e'(r)}}{1+b'(r)\left(1-\frac{\theta}{\pi}\right)^{e'(r)}} \quad (4)$$

where

$$K(r) = K_1 r^{K2} + K_3 r + K_4 \quad (4a)$$
$$a(r) = a_1 r^{a2} + a_3 r + a_4 \quad (4b)$$
$$b(r) = b_1 r^{b2} + b_3 r + b_4 \quad (4c)$$
$$e(r) = e_1 r^{e2} + e_3 r + e_4 \quad (4d)$$
$$a'(r) = a'_1 r^{a'2} + a'_3 r + a'_4 \quad (4e)$$
$$b'(r) = b'_1 r^{b'2} + b'_3 r + b'_4 \quad (4f)$$
$$e'(r) = e'_1 r^{e'2} + e'_3 r + e'_4 \quad (4g)$$

$$g(r) = \frac{hr^i}{1 + jr^K} \quad (5)$$

h, i, j, and k are fitted constants from Monte Carlo data of the Nucletron PDR ^{192}Ir source. Table 1 and 2 show the fitted values of constants reported by Lliso et al. (2001) [10] used for calculating $F(r,\theta)$ and $g(r)$ respectively.

Table 1: Fitted values of constant used for calculating $F(r,\theta)$

i	k_i	a_i	b_i	e_i	a_i'	b_i'	e_i'
1	-1.11182	-	20.054	2.7776	-	21.7092	1.4500
2	-3.6513×10^{-2}	-	1.222×10^{-1}	-8.33×10^{-3}	-	-3.363×10^{-3}	1.0019
3	1.356×10^{-2}	-5.645×10^{-1}	-5.77×10^{-1}	-	3.907×10^{-3}	-4.9914×10^{-2}	-1.3904
4	1.55792	16.958	11.714	-1.0391	5.838×10^{-2}	-22.3700	5.650×10^{-1}

Table 2: Fitted values of constant used for calculating $g(r)$.

parameters	h	i	j	k
value	1.0001	7.30×10^{-3}	8.94×10^{-5}	3.235

By means of Excel Spread sheet, the analytically fitted formulae were used to calculate $F(r,\theta)$ and $g(r)$ for the desired point of dose calculations in the vicinity of the Nucletron PDR ^{192}Ir cylindrical source. The values of $f(r,\theta)$ were calculated for the range $(0.25\,cm \le r \le 10\,cm)$ from the active source centre, and for $0^0 \le \theta \le 180^0$ in the intervals of 10° using the Excel spread sheet. This was to serve as a benchmark for the fitted parameters.

The new hybridized function f(r, θ) has both radial and angular components. This suggests that a strong correlation exists between f(r, θ) and the anisotropy function F(r, θ).
A statistical variable is therefore introduced to link f(r, θ) and F(r, θ) as presented by Acquah et al. (2012) [9] in equation 6.

$$\Delta f' = F(r,\theta) - f(r,\theta) \tag{6}$$

Equation 6 can be rewritten as:

$$f(r,\theta) = F(r,\theta) - \Delta f' \tag{7}$$

Substituting equation 4 into 7,

$$f(r,\theta) = K(r) + \frac{a(r)\left(\frac{\theta}{\pi}\right)^{e(r)}}{1+b(r)\left(\frac{\theta}{\pi}\right)^{e(r)}} + \frac{a'(r)\left(1-\frac{\theta}{\pi}\right)^{e'(r)}}{1+b'(r)\left(1-\frac{\theta}{\pi}\right)^{e'(r)}} - \Delta f' \tag{8}$$

Equation 8 can further be written as:

$$f(r,\theta) = \Delta f + \frac{a(r)\left(\frac{\theta}{\pi}\right)^{e(r)}}{1+b(r)\left(\frac{\theta}{\pi}\right)^{e(r)}} + \frac{a'(r)\left(1-\frac{\theta}{\pi}\right)^{e'(r)}}{1+b'(r)\left(1-\frac{\theta}{\pi}\right)^{e'(r)}} \tag{9}$$

where

$$\Delta f = K(r) - \Delta f' \tag{10}$$

Once more, equation 10 is used here to reduce the number of parameters, and the radial dependence is also catered for. As a result, Δf was treated as a secondary influence on the TG 43 formalism, which then causes it to deviate slightly. The functional fitting focuses on Δf being appended to the truncated form of the Lliso et al formulation. The corresponding values of Δf were then obtained using the MS Excel tool, and the results were tabulated.

Table 3 shows the corresponding values of Δf for $(0.25\,cm \le r \le 10\,cm)$.

ISSN 2224-3577

International Journal of Science and Technology

http://www.ejournalofsciences.org

Table 3: The calculated values of Δf used for the functional fitting at $(0.25cm \le r \le 10cm)$

	Distance from Active Source Centre, r(cm)											
θ°	**0.25**	**0.5**	**1**	**2**	**3**	**4**	**5**	**6**	**7**	**8**	**9**	**10**
0	0.38532	0.42122	0.45967	0.50393	0.53402	0.55692	0.57405	0.58528	0.58963	0.58463	0.56090	0.33278
10	0.38231	0.41968	0.45967	0.50514	0.53531	0.55747	0.57315	0.58252	0.58531	0.58126	0.57029	0.55264
20	0.38242	0.41974	0.45967	0.50509	0.53526	0.55745	0.57319	0.58261	0.58547	0.58146	0.57051	0.55284
30	0.38248	0.41977	0.45967	0.50507	0.53523	0.55744	0.57320	0.58265	0.58552	0.58153	0.57058	0.55291
40	0.38251	0.41978	0.45967	0.50505	0.53522	0.55743	0.57321	0.58267	0.58555	0.58157	0.57062	0.55294
50	0.38253	0.41980	0.45967	0.50504	0.53521	0.55743	0.57321	0.58268	0.58557	0.58159	0.57064	0.55296
60	0.38255	0.41981	0.45967	0.50504	0.53520	0.55743	0.57321	0.58269	0.58558	0.58160	0.57066	0.55297
70	0.38256	0.41981	0.45967	0.50503	0.53520	0.55742	0.57322	0.58270	0.58559	0.58161	0.57067	0.55298
80	0.38257	0.41982	0.45967	0.50503	0.53520	0.55742	0.57322	0.58270	0.58560	0.58162	0.57067	0.55299
90	0.38258	0.41982	0.45967	0.50502	0.53519	0.55742	0.57322	0.58271	0.58560	0.58163	0.57068	0.55299
100	0.38259	0.41983	0.45967	0.50502	0.53519	0.55742	0.57322	0.58271	0.58561	0.58163	0.57069	0.55300
110	0.38260	0.41983	0.45967	0.50502	0.53519	0.55742	0.57322	0.58271	0.58561	0.58164	0.57069	0.55300
120	0.38260	0.41983	0.45967	0.50502	0.53519	0.55742	0.57322	0.58271	0.58562	0.58164	0.57069	0.55300
130	0.38261	0.41984	0.45967	0.50501	0.53519	0.55742	0.57322	0.58272	0.58562	0.58164	0.57069	0.55300
140	0.38261	0.41984	0.45967	0.50501	0.53518	0.55742	0.57322	0.58272	0.58562	0.58164	0.57070	0.55301
150	0.38261	0.41984	0.45967	0.50501	0.53518	0.55742	0.57322	0.58272	0.58562	0.58165	0.57070	0.55301
160	0.38262	0.41984	0.45967	0.50501	0.53518	0.55742	0.57322	0.58272	0.58562	0.58165	0.57070	0.55301
170	0.38262	0.41984	0.45967	0.50501	0.53518	0.55742	0.57323	0.58272	0.58562	0.58165	0.57070	0.55301
180	0.38262	0.41984	0.45967	0.50501	0.53518	0.55742	0.57323	0.58272	0.58563	0.58165	0.57070	0.55301

For the fitting of the Δf data, an objective function has been defined as follows:

$$F_{obj} = \sum_{i=1}^{N} W_i \left[F_{fit}(A, B, C, ..., \theta_i, r_i) - F_{data}(\theta_i, r_i) \right]^2 \quad (11)$$

W_i being a weighting factor, $F_{fit}(A, B, C, ..., \theta_i, r_i)$ is the selected functional form for Δf, $(A, B, C, ...)$ are the parameters, (θ_i, r_i) is the variables of θ and r and F_{data} is the data which the functional form was fitted to, for both radial ranges. The unknown coefficients were computed by doing a least squares fit, which minimizes the sum of the squares of the deviations of the data from the model. This was done to determine the best function that would describe the observed pattern of the plotted data. This function would then be used to model the data.

The appropriate parameters were then fitted by varying the parameters using the Matlab curve fitting tool such that the R^2 value is as closer to 1 as possible (that is $R^2 \approx 1$) and the Root Mean Square Error (RMSE) value as closer to zero (0) as possible.

The fitting made use of non-linear least square fit method, which employed very few parameters combining both exponential and second order polynomial. The functional form which suits the data was obtained as follows:

$$\Delta f = Ar \exp(ar) + Br^2 \exp(br) + C \quad (12)$$

The fitting of Δf was produced for $(0.25cm \le r \le 10cm)$ using Matlab's non-linear least squares. In order to obtain the best fit, the weighting factors were initially set to zero (0), after which they were varied between zero (0) and one (1). The goodness of the fit ensured that $R^2 \approx 1$ and RMSE is as close to zero as possible.

In order to validate the accuracy of the fit functional form, the dose rate distributions of the source $\dot{D}(r, \theta)$ per unit air kerma strength were reproduced for the radial range $(0.25cm \le r \le 10cm)$ from the active core, at $0^0 \le \theta \le 180^0$. This was obtained using the TG 43 formalism, the fit functional form obtained in equation 12, the published dose rate constant (Λ) and the geometrical factor of the TG 43. Hence, the equation employed in the calculation of $\dot{D}(r, \theta)$ was given as:

$$\dot{D}(r, \theta) = S_K \Lambda \frac{1}{r^2} f(r, \theta) \quad (13)$$

where

$$f(r, \theta) = K(r) - \Delta f - F(r, \theta) \quad (14)$$

where Λ= dose-rate constant for the source and surrounding medium [cGy/h/U] (1U= 1 cGy/cm^2/h), $f(r, \theta)$ is the hybridized form of g(r) and F(r,θ) shown in equation 3. For the microSelectron PDR source, the value of Λ in water is 1.121 cGy/h/U. However, in the AAPM TG 43, the recommended value for Λ in water is the round off of 1.121, which is 1.12. In practice, the TG 43 formalism uses a line source model for the geometric factor, but the point source model ($1/r^2$) is used here for the purpose of easy comparison. This development was done to compare the dose rate obtained by Lliso et al. (2001) [10]. to that obtained in this work. The deviation between the two was considered as errors in the dose distribution, taking the fit of Lliso et al. (2001) [10] as a reference.

The deviations were therefore calculated as follows:

$$Deviation = \dot{D}(r, \theta)_{this\_work} - \dot{D}(r, \theta)_{Lliso} \quad (15)$$

where $\dot{D}(r, \theta)_{this\_work}$ is the dose rate distribution obtained in this study.

$\dot{D}(r, \theta)_{Lliso}$ is the dose rate obtained in Lliso's study.

In order to evaluate the error margins obtained in this study, the percentage errors for each data point was obtained in equation 15 as follows:

$$E = \frac{\Delta f_{fit} - \Delta f_{Lliso}}{\Delta f_{Lliso}} \times 100\% \quad (16)$$

where

Δf_{fit} is Δf obtained in this work.

Δf_{Lliso} is Δf obtained from the work of Lliso.

The average percentage error for angle (θ°) was also obtained as follows:

$$E_{avg} = \frac{1}{N} \sum_{i}^{N} \left| \frac{\Delta f_{fit} - \Delta f_{Lliso}}{\Delta f_{data}} \right| \times 100\% \quad (17)$$

where N is the data size.

To check the error margins in the absolute dose calculations obtained in this work, the percentage errors for each data point was obtained as follows:

$$E = \frac{\dot{D}(r,\theta)_{this\_work} - \dot{D}(r,\theta)_{Lliso}}{\dot{D}(r,\theta)_{Lliso}} \times 100\,\% \qquad (18)$$

Where $\dot{D}(r,\theta)_{Lliso}$ and $\dot{D}(r,\theta)_{this\_work}$ are obtained from Lliso's study and this study respectively.

III. RESULTS

Tables 4 and 5 are the calculated values of Δf derived from Lliso's work and this work (fit for range $0.25\,cm \le r \le 10\,cm$) respectively. At each angle, the calculated Δf derived from Lliso's work is compared to that of this work. An average percentage error is observed and is clearly shown in Table 5 for angle 40^0. A greater percentage error of $0.96\,\%$ is seen at angle 0^0. However, above 0^0, the average discrepancy is seen to be below $0.25\,\%$. For example, the Δf obtained from the fit at polar angles 10^0, 20^0 and 60^0 differed by as low as 0.24 $\%$. This is demonstrated in Tables 5 and 6 for angles 40^0 and 60^0 respectively.

Table 4: Comparison of Δf obtained for polar angle 20^0 at $0.25\,cm \le r \le 10\,cm$.

Polar angle (θ = 20°)				
r(cm)	Δf_{Lliso} (y_1)	Δf_{fit} (y_2)	Deviation $(y_2 - y_1)$	percentage error E
0.25	0.382420	0.383746	0.001326	0.346739
0.50	0.419740	0.417056	-0.002680	-0.638490
1.00	0.459670	0.460930	0.001260	0.274110
2.00	0.505090	0.506045	0.000955	0.189075
3.00	0.535260	0.533914	-0.001350	-0.252210
4.00	0.557450	0.556655	-0.000790	-0.141720
5.00	0.573190	0.573877	0.000687	0.119856
6.00	0.582610	0.583767	0.001157	0.198589
7.00	0.585470	0.585736	0.000266	0.045434
8.00	0.581460	0.580454	-0.001010	-0.173700
9.00	0.570510	0.569314	-0.001200	-0.210340
10.00	0.552840	0.553955	0.001115	0.201686

$$E_{avg} = 0.235478\%$$

Table 5: Comparison of Δf obtained for polar angle 40^0 at $0.25\,cm \le r \le 10\,cm$.

Polar angle (θ = 60°)				
r(cm)	Δf_{Lliso} (y_1)	Δf_{fit} (y_2)	Deviation $(y_2 - y_1)$	percentage error E
0.25	0.382550	0.383895	0.001345	0.351588
0.50	0.419810	0.417156	-0.002650	-0.631240
1.00	0.459670	0.460951	0.001281	0.278678
2.00	0.505040	0.506000	0.000960	0.190084
3.00	0.535200	0.533888	-0.001310	-0.244770
4.00	0.557430	0.556681	-0.000750	-0.134550
5.00	0.573210	0.573956	0.000746	0.130144
6.00	0.582690	0.583889	0.001199	0.205770
7.00	0.585580	0.585888	0.000308	0.052597
8.00	0.581600	0.580625	-0.000980	-0.168500
9.00	0.570660	0.569498	-0.001160	-0.203270
10.00	0.552970	0.554146	0.001176	0.212670

$$E_{avg} = 0.248553\%$$

Table 6: Comparison of Δf obtained for polar angle 60^0 at $0.25\,cm \le r \le 10\,cm$.

Polar angle (θ = 40°)				
r(cm)	Δf_{Lliso} (y_1)	Δf_{fit} (y_2)	Deviation $(y_2 - y_1)$	percentage error E
0.25	0.382510	0.384035	0.001525	0.398682
0.50	0.419780	0.416971	-0.002810	-0.669400
1.00	0.459670	0.460883	0.001213	0.263885
2.00	0.505050	0.506294	0.001244	0.246312
3.00	0.535220	0.534000	-0.001220	-0.227940
4.00	0.557430	0.556633	-0.000800	-0.143520
5.00	0.573210	0.573942	0.000732	0.127702
6.00	0.582670	0.583966	0.001296	0.222424
7.00	0.585550	0.585986	0.000436	0.074460
8.00	0.581570	0.580662	-0.000910	-0.156470
9.00	0.570620	0.569464	-0.001160	-0.203290
10.00	0.552940	0.554125	0.001185	0.214309

$$E_{avg} = 0.235563\%$$

Table 7: The calculated values of the absolute dose rate distribution per unit air kerma strength, $\dot{D}(r,\theta)_{fit}$ obtained from our work (fit at radial range $0.25cm \le r \le 10cm$)

	Distance from Active Source Centre, r(cm)											
θ°	**0.25**	**0.5**	**1**	**2**	**3**	**4**	**5**	**6**	**7**	**8**	**9**	**10**
0	11.7514	2.834399	0.71451	0.188568	0.088056	0.051552	0.034131	0.024503	0.018758	0.015353	0.014018	0.028285
10	16.85252	4.218969	1.066422	0.268978	0.120015	0.067777	0.04343	0.030024	0.021803	0.016384	0.012627	0.009925
20	16.65793	4.167044	1.052944	0.265719	0.118705	0.06714	0.04309	0.029834	0.021696	0.016324	0.012594	0.009909
30	16.5626	4.141763	1.046471	0.264221	0.118131	0.066874	0.042956	0.029763	0.021657	0.016303	0.012583	0.009904
40	16.50725	4.12550	1.042477	0.263409	0.117811	0.066721	0.042882	0.029728	0.02164	0.016294	0.012578	0.009902
50	16.46385	4.115568	1.039852	0.262733	0.117579	0.066628	0.042835	0.029701	0.021625	0.016286	0.012575	0.00990
60	16.43354	4.107586	1.037868	0.262298	0.117424	0.066559	0.042802	0.029684	0.021616	0.016282	0.012573	0.009899
70	16.4137	4.100788	1.036273	0.26204	0.117313	0.066503	0.042776	0.029674	0.021612	0.016279	0.012571	0.009898
80	16.39081	4.09639	1.035089	0.261697	0.117209	0.066466	0.042758	0.029662	0.021605	0.016276	0.01257	0.009898
90	16.37889	4.091668	1.034007	0.261554	0.117142	0.066429	0.042742	0.029657	0.021603	0.016275	0.012568	0.009897
100	16.36353	4.089197	1.033318	0.261328	0.117082	0.066415	0.042736	0.029652	0.021601	0.016274	0.012569	0.009898
110	16.35205	4.086193	1.032589	0.261173	0.11703	0.066393	0.042725	0.029647	0.021598	0.016273	0.012569	0.009898
120	16.34217	4.083624	1.031951	0.261039	0.116982	0.066374	0.042716	0.029643	0.021596	0.016272	0.012568	0.009897
130	16.33507	4.080135	1.031159	0.260952	0.116931	0.06634	0.042699	0.029635	0.021592	0.016268	0.012565	0.009895
140	16.32529	4.079122	1.030857	0.260812	0.116906	0.066343	0.042702	0.029636	0.021593	0.01627	0.012567	0.009897
150	16.31864	4.077463	1.030449	0.260729	0.116878	0.06633	0.042697	0.029633	0.021591	0.01627	0.012567	0.009897
160	16.3120	4.075651	1.030005	0.260636	0.116847	0.066318	0.042692	0.029631	0.02159	0.016269	0.012567	0.009897
170	16.30628	4.074189	1.029658	0.260568	0.116825	0.06631	0.042688	0.029629	0.021589	0.016269	0.012567	0.009897
180	16.30106	4.072826	1.029321	0.260499	0.116801	0.06630	0.042684	0.029627	0.021588	0.016268	0.012566	0.009896

Table 7 shows the absolute dose rate distribution values calculated in this work from the fit using the radial range of $0.25cm \le r \le 10cm$. The values are compared with the absolute dose rate values obtained from Lliso's work. The findings show these values are in fair agreement to each other, with a maximum percentage error of 0.3 %. Examples are shown in Tables 8 and 9.

Table 8: Comparison of $\dot{D}(r,\theta)$ date for the fit of Lliso with $\dot{D}(r,\theta)$ proposed in this work for the radial range $0.25cm \le r \le 10cm$ at 20^0.

Polar angle (θ = 20°)				
r(cm)	$\dot{D}(r,\theta)_{Lliso}$ (y_1)	$\dot{D}(r,\theta)_{this\_work}$ (y_2)	Deviation $(y_2 - y_1)$	percentage error E
0.25	16.634200	16.657900	0.023720	0.142598
0.50	4.179080	4.167040	-0.012030	-0.287890
1.00	1.051530	1.052940	0.001412	0.134280
2.00	0.265450	0.265720	0.000268	0.100960
3.00	0.118870	0.118710	-0.000170	-0.140490
4.00	0.067200	0.067140	-5.5×10^{-05}	-0.081850
5.00	0.043060	0.043090	3.1×10^{-05}	0.071994
6.00	0.029800	0.029830	3.6×10^{-05}	0.120813
7.00	0.021690	0.021700	6×10^{-06}	0.027663
8.00	0.016340	0.016320	-1.8×10^{-05}	-0.110150
9.00	0.012610	0.012590	-1.7×10^{-05}	-0.134800
10.00	0.009900	0.009910	1.2×10^{-05}	0.121249

$$E_{avg} = 0.122894\%$$

Table 9: Comparison of $\dot{D}(r,\theta)$ date for the fit of Lliso with $\dot{D}(r,\theta)$ proposed in this work for the radial range $0.25cm \le r \le 10cm$ at 180^0

Polar angle (θ = 180°)				
r(cm)	$\dot{D}(r,\theta)_{Lliso}$ (y_1)	$\dot{D}(r,\theta)_{this\_work}$ (y_2)	Deviation $(y_2 - y_1)$	percentage error E
0.25	16.27690	16.30110	0.024140	0.148308
0.50	4.084660	4.072830	-0.011840	-0.289820
1.00	1.027880	1.029320	0.001442	0.140289
2.00	0.260230	0.260500	0.000270	0.103755
3.00	0.116960	0.116800	-0.000160	-0.139360
4.00	0.066350	0.066300	-5.1×10^{-05}	-0.076860
5.00	0.042650	0.042680	3.5×10^{-05}	0.082065
6.00	0.029590	0.029630	3.8×10^{-05}	0.128426
7.00	0.021580	0.021590	7×10^{-06}	0.032436
8.00	0.016290	0.016270	-1.7×10^{-05}	-0.104390
9.00	0.012580	0.012570	-1.6×10^{-05}	-0.127170
10.00	0.009880	0.009900	1.3×10^{-05}	0.131539

$$E_{avg} = 0.125368\%$$

In Figure 2, a graph of the absolute dose rate $\dot{D}(r,\theta)$ calculated for polar angle 40^0 taken is plotted for the range $0.25\,cm \le \theta \le 10\,cm$ from the active source. Between distances of 0 to 2 cm from the active source centre, a steep fall in the dose rate is observed. However, beyond 2 cm some differences were seen. The dose rate distribution decreased steadily. This steep dose gradients near the source explains the contribution to the dose rate by beta particles emitted by ^{192}Ir, and the contribution of the conversion electrons that are emitted from the unencapsulated ends of the Nucletron ^{192}Ir PDR seed.

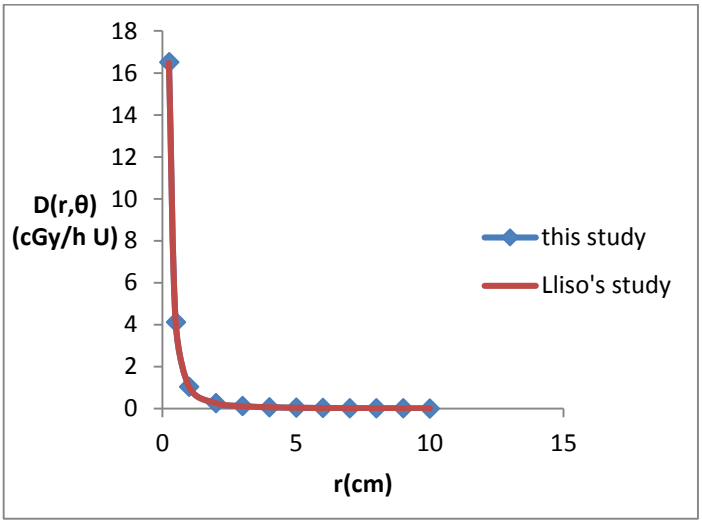

Figure 2: Graph of Dose rate per unit air-kerma strength (in cGy h^{-1} U^{-1}) obtained at angle 40^0 for $0.25\,cm \le r \le 10\,cm$. The data by this study are indicated by blue diamonds and that for Lliso et al. are indicated red line respectively.

IV. DISCUSSION

With the introduction of the hybridization of the radial and anisotropy factors, the number of parameters has reduced. As a consequence, this has made the dose rate calculations much easier and faster. Interestingly, the interpolation and extrapolation of the simple hybridized function f(r, θ) in the treatment planning is a forward-looking technique, and a relatively simple method than the inept method of combining separate tables of the radial and anisotropy factors.

Each dose rate value obtained in this study is however subject to some discrepancies as shown in Table 10 for angle 20^0.

Table 10: Evaluation of the dose rate per unit air-kerma strength (in $cGyh^{-1}U^{-1}$) obtained at angle 20^0.

Polar angle (θ = 20°)				
r(cm)	$\dot{D}(r,\theta)_{Lliso}$ (y_1)	$\dot{D}(r,\theta)_{this\_work}$ (y_2)	**Deviation** $(y_2 - y_1)$	**percentage error** E
0.25	16.634200	16.657900	0.023720	0.142598
0.50	4.179080	4.167040	-0.012030	-0.287890
1.00	1.051530	1.052940	0.001412	0.134280
2.00	0.265450	0.265720	0.000268	0.100960
3.00	0.118870	0.118710	-0.000170	-0.140490
4.00	0.067200	0.067140	-5.5×10^{-05}	-0.081850
5.00	0.043060	0.043090	3.1×10^{-05}	0.071994
6.00	0.029800	0.029830	3.6×10^{-05}	0.120813
7.00	0.021690	0.021700	6×10^{-06}	0.027663
8.00	0.016340	0.016320	-1.8×10^{-05}	-0.110150
9.00	0.012610	0.012590	-1.7×10^{-05}	-0.134800
10.00	0.009900	0.009910	1.2×10^{-05}	0.121249

$$E_{avg} = 0.122894\,\%$$

In this particular study, the uncertainties in the dose rates have been evaluated according to the recommendation of the TG 43 protocol. In an example at angle 20^0, there is an average discrepancy of 0.12%. However, entirely at the top of the source ($\theta = 0^0$), the discrepancy is maximum (Table 11). Such a discrepancy at 0^0 could possibly be due to several factors and uncertainties such as the contribution of beta particles emitted by ^{192}Ir, and the contribution of the conversion electrons that are emitted from the unencapsulated ends of the Nucletron ^{192}Ir PDR seed to the dose rate at distances very close to the longitudinal axis of the source.

Table 11: Evaluation of the dose rate per unit air-kerma strength (in $cGyh^{-1}U^{-1}$) obtained at angle 0^0.

Polar angle (θ = 0°)				
r(cm)	$\dot{D}(r,\theta)_{Lliso}$ (y_1)	$\dot{D}(r,\theta)_{this\_work}$ (y_2)	**Deviation** $(y_2 - y_1)$	**percentage error** E
0.25	11.472000	11.751400	0.279390	2.435406
0.50	2.848220	2.834400	-0.013820	-0.485220
1.00	0.726370	0.714510	-0.011860	-1.632910
2.00	0.190090	0.188570	-0.001520	-0.798590
3.00	0.088060	0.088060	1×10^{-06}	0.001136
4.00	0.051450	0.051550	0.000103	0.200198
5.00	0.034140	0.034130	-5×10^{-06}	-0.014650
6.00	0.024590	0.024500	-8.7×10^{-05}	-0.353800
7.00	0.018850	0.018760	-9.6×10^{-05}	-0.509180
8.00	0.015390	0.015350	-3.8×10^{-05}	-0.246900
9.00	0.014070	0.014020	-4.7×10^{-05}	-0.334160
10.00	0.028270	0.028290	1.1×10^{-05}	0.038905

$$E_{avg} = 0.587587\,\%$$

Nevertheless, these errors obtained at each fixed angle are well within the statistical uncertainty limit recommended by the protocol. The dose rate uncertainties obtained in this work are far less than 1%. The protocol recommends a statistical uncertainty limit $\leq 2\,\%$ for distances less than 5 cm [11], which implies a higher degree of accuracy in the dose rate has been achieved in this work. Again, this high degree of accuracy is displayed in figure 2. The diagram shows that the absolute dose rate distribution calculated from the work of Lliso is in strong agreement with that obtained in this study.

The results show the fitting errors in Δf are not clinically relevant in dose calculations. This could probably be due to the indirect relation between the dose rate and Δf. In contrast, f(r, θ) directly relates to the dose rate distribution, and contributes directly to the errors in the calculation of dose in the treatment planning system. Thus, the absolute dose rate calculations per unit air kerma strength obtained behaved as f(r, θ), demonstrating similar discrepancies.

In this study, very small emphasis is however made on the angular dependence of f(r, θ) in the new function. The dependence of f(r, θ) is not fully integrated in the new function, and although as the present data show, future work is needed to address this issue.

REFERENCES

[1] ESTRO, A practical guide to quality control of brachytherapy equipment, booklet no.8. Pp 125-132 (2004).

[2] P. mayles, A Nahum, C. Rosenwald. Handbook of Radiotherapy physics (Theory and Practice). Pp 1101 – 1107, 1135, 36 (2007).

[3] D. Berger, J. Dimopoulos, P. Georg, D. George, R. Potter, Kirisits C. Uncertainties in assessment of the vaginal dose for intracavitary brachytherapy of cervical cancer using a tandem-ring applicator. Int J Radiation Oncology Biol Phys. Feb Apr 1; 67(5): pp 1451-9 (2007).

[4] P. Wexberg, C. Kirisits, D. Berger, I. Sulzbacher, G. Maurer, R. Potter, D. Georg, D. Glogar. Quantification of dose perturbation by plaque in vascular brachytherapy. Mar; 35(3): pp180-5 (2005).

[5] J. F. Williamson and Z. Li. Monte Carlo aided dosimetry of the microselectron pulsed and high dose-rate ^{192}Ir sources. Med. Phys. 22, 809–819 (1995).

[6] R. Nath, L. L. Anderson, G. Luxton, K. A. Weaver, J. F. Williamson, and A. S. Meigooni. Dosimetry of interstitial brachytherapy sources: Recommendations

of the AAPM Radiation Therapy Committee Task Group No. 43. Med. Phys. 22, 209–234 (1995).

[7] R. Wang and R. Svoboda. Monte Carlo dosimetry of the Varisource high dose-rate ^{192}Ir source. Med. Phys. 25, 415–423 (1998).

[8] G. M. Daskalov, E. Loffler, and J. Williamson. Monte Carlo aided dosimetry of a new high dose-rate brachytherapy source. Med. Phys. 25, 2200–2208 (1998).

[9] G.F. Acquah, E.K. Nani, E.K.T. Addison, S.N. Tagoe, P.O. Kyeremeh, E.K. Sosu and F. Hasford. Fitting and Benchmarking of Monte Carlo Output Parameters for 192Ir High Dose Rate Brachytherapy "New or v2" Source. International Journal of Science and Technology, ISSN 2224-3577, (2012).

[10] F. Lliso, F.Ballester, J. Pérez-Calatayud, , V. Carmona, J. L. Lluch, , M. A Serrano., Y. Limami, and E. Casal. Fitted dosimetric parameters of high dose-rate 192 Ir sources according to the AAPM TG 43 formalism. Phys. Med. Biol., (2001).

[11] Yves Lemigne, Alessandra Caner. Radiotherapy and Brachytherapy. Pp 186, 189, 192 240 and 246 (2007).